Linker Dependent Bond Rupture Force Measurements in Single-Molecule Junctions

Michael Frei,[†] Sriharsha V. Aradhya,[†] Mark S. Hybertsen,*[‡] and Latha Venkataraman*[†]

[†]Department of Applied Physics and Applied Mathematics, Columbia University, New York, New York 10027, United States
[‡]Center for Functional Nanomaterials, Brookhaven National Laboratories, Upton, New York 11973, United States

S *Supporting Information*

ABSTRACT: We use a modified conducting atomic force microscope to simultaneously probe the conductance of a single-molecule junction and the force required to rupture the junction formed by alkanes terminated with four different chemical link groups which vary in binding strength and mechanism to the gold electrodes. Molecular junctions with amine, methylsulfide, and diphenylphosphine terminated molecules show clear conductance signatures and rupture at a force that is significantly smaller than the measured 1.4 nN force required to rupture the single-atomic gold contact. In contrast, measurements with a thiol terminated alkane which can bind covalently to the gold electrode show conductance and force features unlike those of the other molecules studied. Specifically, the strong Au−S bond can cause structural rearrangements in the electrodes, which are accompanied by substantial conductance changes. Despite the strong Au−S bond and the evidence for disruption of the Au structure, the experiments show that on average these junctions also rupture at a smaller force than that measured for pristine single-atom gold contacts.

Electronic properties of single-molecule circuits have been probed extensively, providing insight into junction formation and structure.[1] However, conductance data alone is often insufficient to fully explain the complex, atomic processes that control the evolution of the junction structure, in particular under stress. We have recently developed a method to measure and analyze simultaneously force and conductance of these single-molecule junctions.[2] The force measurements can be used to determine bond rupture forces, junction stiffness, and their relation to the loading rate,[3] thus providing characteristic force signature for particular bond rupture events occurring during junction formation and evolution. Here, we present a study of conductance and breaking force measurements on a series of single-molecule junctions with four different linker groups: amine, methylsulfide, diphenylphosphine, and thiol. For the first three, which bind to gold through a donor−acceptor (D−A) bond, we see a clear conductance signature with junctions rupturing under 0.6−0.8 nN stress. In contrast, junctions with thiol linkers undergo multiple plastic deformation events during elongation, indicative of structural rearrangements. However, we find that these events, including the terminal event indicative of final junction rupture, have an average force that is smaller than the 1.4 nN observed for the

rupture force of a single Au atom contact. These results show that the rupture of a Au−S bonded junction, which would most likely occur at a Au−Au bond, does not require a force of 1.4 nN contrary to what is commonly assumed.

We use a modified conductive atomic force microscope (AFM) to investigate the breaking mechanism of single-molecule junctions formed with different linker groups. The experimental methods have been described previously.[2] Briefly, a gold coated cantilever and a gold-on-mica substrate are repeatedly brought in and out of contact using a high resolution piezoelectric positioner (schematic SI Figure S1). Conductance is measured across the tip/sample junction at constant bias. The force is measured simultaneously by monitoring the deflection of a laser focused on the back of the cantilever. In the absence of molecules clean Au−Au point contacts are formed and broken. A conductance trace (Figure 1A) shows a typical
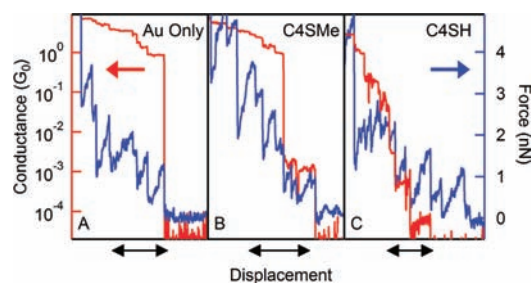
Figure 1. Sample conductance (red) and force (blue) traces for Au only (A), C4SMe (B), and C4SH (C). Arrow indicates a 0.5 nm displacement.

stepwise decrease in conductance as a function of displacement. The simultaneously measured force traces show a sawtooth pattern attributed to reversible (elastic) and irreversible (plastic) deformations during conductance plateaus and drops respectively.[4] When Au point contacts are broken in the presence of molecules, additional features are seen in the conductance and force traces (Figure 1B, C). The conductance of a single-molecule junction and the force required to rupture this junction can be determined from these simultaneously acquired data.

In this work, we investigate how single-molecule junction rupture forces correlate with the molecular link chemistry. Since measured rupture forces for the Au−N donor−acceptor
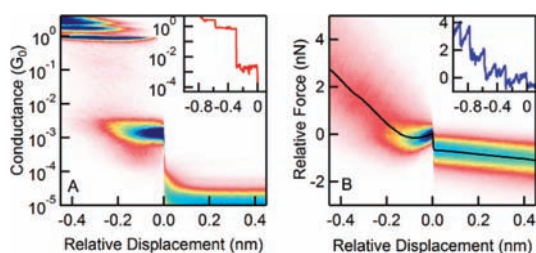
bond depend on the molecular backbone,[2] we focus here on measurements of alkane backbones terminated with different linkers. Specifically we compare bond rupture forces in junctions formed with 1,4-butanediamine (C4NH2), 1,4-bis(methylsulfide) butane (C4SMe), 1,5 bis-(diphenylphosphino)pentane (C5DPP), and 1,4-butanedithiol (C4SH). All these compounds are obtained from commercial sources and used without further purification. The amine (NH$_2$), methylsulfide (SMe), and diphenylphosphine (DPP) linkers bind to gold through a D−A bond[5] while the thiol linker can form a covalent bond with the Au electrodes displacing the H. In the experiments, the molecules are deposited onto the Au substrate by either evaporation or addition of a dilute concentration of molecule in the solvent 1,2,4-trichloroben-zene (TCB). Both conductance and force results are independent of the deposition method.

Figure 1B shows a typical, single conductance (red) and force (blue) measurement for C4SMe. In addition to the gold features at and above 1G$_0$ we can now also identify a molecular conductance plateau at ~10^{-3} G$_0$. In the simultaneously measured force trace, two additional sawtooth patterns are seen within the step, followed by the final rupture, coinciding with the end of the conductance plateau. This trace indicates that this single-molecule junction underwent some structural rearrangements before being ruptured. Sample conductance and force traces for C4NH$_2$ and C5DPP have similar features, although the magnitude of the conductance at the plateaus and the forces are molecule dependent. In contrast, however, the conductance traces for measurements with C4SH are quite different (Figure 1C). We do not see a clear conductance plateau, and multiple sawtooth events are seen in the force trace after the single Au point-contact is broken, corresponding to a range of conductance values, down to the measurement limit of 2×10^{-5}G$_0$. We will return to a discussion of this data set below.

To determine, with statistical significance, junction conductance and bond rupture forces, we collect thousands of simultaneous conductance and force traces for each molecule on multiple tip/sample pairs. For C4NH$_2$, C4SMe, and C5DPP, these large data sets are analyzed by using a 2D histogram technique, detailed previously[2] and shown in Figure 2 (details in Supporting Information (SI)). To determine the

rupture force. For measurements with clean gold, the rupture force of a G$_0$ conductance junction is determined to be 1.4 nN (SI Figure S4), consistent with previous results.[6] The same methodology is applied to evaluate junction rupture force for Au-molecule-Au junctions with NH$_2$, SMe, and DPP linker groups.

Figure 2A shows a 2D conductance histogram of C4SMe measurements. This histogram is constructed from 9774 traces similar to those shown in Figure 1B and the inset of Figure 2A. The histogram is constructed using logarithmic bins along the y-axis and linear bins along the x-axis. All traces in this histogram are aligned such that zero displacement is right after the molecular conductance plateau. The subset of measured traces that do not show molecular conductance plateaus are excluded; these histograms are created using 9774 traces out of 27000 traces measured. A prominent peak at G$_0$ is visible and is offset from a single, well-defined conductance peak centered at ~10^{-3}G$_0$ along the conductance axis, indicating the 1G$_0$ plateau occurs before molecular junctions are formed. The molecular step extends from −0.3 to 0 nm along the displacement axis, consistent with previous measurements.[5] SI Figures S5A−S6A show the 2D conductance histograms for measurements with C4NH$_2$ and C5DPP.

Figure 2B shows the 2D force histogram for C4SMe constructed from the simultaneously measured 9774 force traces corresponding to the conductance traces used to generate the histogram in Figure 2A. The force profile (black line) indicates an average breaking force of 0.7 nN for a C4SMe. The force histograms for C4NH$_2$ (SI Figure S5B) and C5DPP (SI Figure S6B) indicate an average breaking force of 0.6 and 0.8 nN respectively. For these three linker groups, we see that the bond rupture force is much smaller than that associated with breaking the Au point contact with 1G$_0$ conductance. It is most likely that these junctions break at the Au−N, Au−S, or Au−P donor−acceptor bonds respectively.[2,5b,7]

For comparison, we use density functional theory based calculations[8] to estimate the maximum sustainable force for each link bond. As described previously and in the SI,[2] a model structure is adiabatically elongated. The prior result for a representative C4NH$_2$ junction was 0.84 nN, and the present result for a C4SMe junction with the same overall structure is also 0.84 nN (SI Figure S9), with rupture occurring at the Au−N and Au−S bond respectively. In a real junction, the orientation of the link bond and the details of the Au atomic scale structure near the link vary, affecting the binding energy and the maximum force[7] suggesting good quantitative agreement with experiment. Interestingly, similar calculations of the maximum sustained force for the Au−P donor−acceptor bond was found to be ~1.5 nN for the dimethylphosphine linker, with clear indications that the stress was sufficient to rearrange the local Au atomic arrangement near the link bond.[5b,7] Selectivity of the link bonding motif to specific under-coordinated Au atomic sites still results in the well-defined conductance plateaus. In most of the scenarios simulated, the P−Au bond ultimately ruptured. Modest steps in conductance are often observed in individual experimental traces that may correspond to rearrangement (SI Figure S6A inset). Qualitatively, the DFT-based simulations are consistent with the measurements, but the relatively low measured average rupture force remains a puzzle. One possibility is that constraints in full junction formation (bonds to substrate and tip, accommodating the bulky tertiary phenyl groups) result in structures where the

Figure 2. (A) 2D conductance histogram for C4SMe constructed from 9774 traces, showing a peak at 1G$_0$ and the molecular signature at 1.4 × 10^{-3}G$_0$. Inset: sample conductance trace. (B) 2D force histogram for the simultaneously acquired force traces. The average force profile in black shows an average breaking force of 0.7 nN. Inset: Force trace corresponding to the conductance trace shown in part A.

rupture force, a force profile is obtained by determining the peak of the 2D force histogram cross section at every displacement value. The magnitude of the sharp drop in this profile at zero displacement corresponds to the average bond

4004

dx.doi.org/10.1021/ja211590d | J. Am. Chem. Soc. 2012, 134, 4003−4006

D−A bonds are weaker than optimal. The rearrangement of the local Au atomic structure may also be significant, as discussed below.

Results from measurements with the C4SH differ from those of the other three linkers. We see a multitude of conductance features over a wide range of conductance spanning from just below G_0 to the experimental noise floor.[9] These results are in contrast to the distinct conductance plateaus seen in C4SMe measurements where a D−A bond formed between the S and an undercoordinated Au atom. For the SH linker, there are multiple bonding scenarios for a Au−S covalent bond,[10] many possible locations for the adsorption of the H atom on the electrodes, and also a possibility of forming an Au−SH donor−acceptor bond.

1D conductance histograms, generated from over 10000 traces for both molecules, are shown in SI Figure S7. No clear conductance peak is visible for the C4SH data, which precludes unambiguous assignment of the displacement at which the junction ruptured in each trace, essential input to construct a 2D conductance or force histogram. We therefore focus the analysis on the force traces and use an alternate approach, based on identification of all sharp drops in individual force traces with an automated algorithm (details in the SI). Each force drop can be associated with the conductance of the junction immediately prior to the force event. One key difference between the 2D force analysis technique used above and this alternate force event identification method is that the former relies on the identification of events through conductance and therefore does not bias the results toward larger force values that are more easily identified. In what follows, we compare the results from measurements of C4SH and C4SMe.

Figure 3 shows a 2D histogram of the change in force for each force event against the associated conductance immedi-
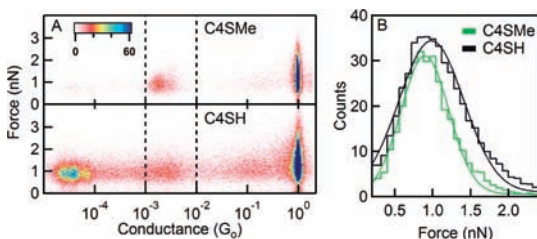

Figure 3. (A) 2D histogram showing all identified force events vs conductance right before the force event for C4SMe (top) and C4SH (bottom). The histograms include 51000 and 121000 individual force events respectively. The conductance bin size is 30 bins per decade, and the force bin size is 0.04 nN. (B) Histogram of force events for C4SMe (green) and C4SH (black) with conductance within the range indicated by dashed lines (10^{-2}−$10^{-3}G_0$).

ately prior to the force event from all measured traces for C4SMe (Figure 3A, top) and C4SH (Figure 3A, bottom). Both histograms show a large number of force events at a conductance value around $1G_0$. These force events correspond to rearrangement and the final breaking of a single-atom gold contact. For C4SH (Figure 3A, bottom), we find numerous force events spread along the conductance axis from just below $1G_0$ to the noise floor of $\sim 2 \times 10^{-5}G_0$ with 75% of all measured traces exhibiting force events with a conductance below $1G_0$. For this selected subset, we find that each trace has an average of 2.7 force events. This is a direct indication that junctions formed with the S−Au bond undergo substantial

rearrangements with varied atomic structure that sustain a broad range of conductance values. In contrast, the C4SMe data show that almost all force events below $1G_0$ occur within a narrowly defined conductance range.[7] Of all the measured traces, 40% show force events for a conductance below $1G_0$, and of this subset, each trace has an average of 1.5 force events. In SMe-terminated molecular junctions, structural rearrangements are not accompanied by large changes in conductance. This agrees with previous DFT based junction elongation simulations[7] that show shifts in attachment point for the D−A bond with modest changes in junction conductance. Finally, the C4SH data also show a significant number of force events with conductance values that are too low to measure in this setup. This could be due to the formation of molecular dimers or due to pulling out of chains of gold atoms, as has been seen in simulations.[11]

Since the broadly distributed conductance values in the C4SH data indicate substantial variation in the Au−S link structure, we plot in Figure 3B a histogram of the force jump for all force events within 10^{-2}−$10^{-3}G_0$. For C4SMe the peak of this distribution occurs at 0.9 nN, which is higher than the force determined from the 2D force histogram analysis method. As discussed above, this selected data set is skewed toward traces that have larger force rupture events. For C4SH, the peak is at 1 nN, very similar to the C4SMe, although the distribution does show a larger number of high force events. One possibility is that for the subset of the C4SH data with this conductance range, the junction is actually formed with a D−A bond to SH, similar to the SMe case (Figure 4A). Our DFT-based
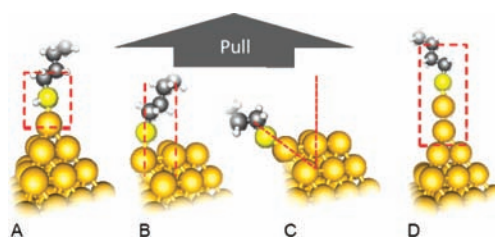
Figure 4. Possible contact structures in single-molecule junctions formed with C4SH. Scenarios: (A) H atom remains on the S; (B) Au atom is not at the apex of the electrode; (C) junction is formed at an angle; (D) Au atom coordination is different.

calculations indicate that such bonds exhibit maximum sustained forces that are very similar (SI Figure S10), in agreement with other calculations for SH.[12]

In fact, the distribution of bond rupture forces does not depend strongly on conductance for C4SH and the histogram of all force events with conductance below 0.1 G_0 is very similar to that shown in Figure 3B. A histogram of the maximal rupture/rearrangement force within each trace with a conductance value below $1G_0$ (SI Figure S8) does show somewhat larger most probable rupture forces (0.9 and 1.2 nN for C4SMe and C4SH respectively). This does suggest that C4SH junctions tend to form links that can sustain a larger force. Still these results imply that rupturing or rearranging the C4SH junction does not, on average, require the 1.4 nN required to rupture the single Au-atom contact.[13]

The measured rupture force for the Au point contact has been a widely used point of reference to distinguish the rupture mechanism between Au-link bond breaking and Au−Au bond breaking. For example previous measurement gave 1.5 nN rupture forces for thiol linked junctions, interpreted to indicate

Au−Au bond breaking in the junction.[13] DFT based calculations indicate that selected scenarios support a maximum sustained Au−S bond force in excess of 1.5 nN.[12] More strikingly, detailed molecular dynamics simulations of thiol-linked junction evolution show a rich series of rupture/rearrangement events with the molecule removing one or more Au atoms in the final, ruptured state.[11] Also, the position and resulting effects of the hydrogen from the SH can lead to drastic changes in force and conductance values.[11c,12,14]

The simultaneous conductance and force trajectories for C4SH junctions, are consistent with a sustained force that is sufficient to drive substantial rearrangement of the local structure during elongation. However, most of these events occur with a change in force that is substantially less than the average force required to rupture the Au point contact. Molecular dynamics simulations illustrate that junctions formed with Au−S links can result in contact structures that have varied geometries and rupture at either Au−link or Au−Au bonds. The terminal Au atom could be on the side of an electrode structure (Figure 4B), the constraints on junction formation with two distinct link bonds, one to each electrode, can result in an angle between the backbone and the pulling direction (Figure 4C), and the coordination of the Au atom to which the S is bonded can be different (Figure 4D). A key factor is the strength of the Au−S bond relative to the softness of the Au resulting in local rearrangement under stress.[11] Calculated adiabatic trajectories for selected scenarios illustrate that the maximum sustained force can be both larger and smaller than the nominal Au point contact rupture force depending on structure (SI Figure S11). A broader-based survey of structure as well as investigation of the role of thermal fluctuations and solvent interactions will be essential to fully understand the measured rupture forces in cases like thiol bonded junctions with strong bonds to Au.

In conclusion, we presented simultaneous force and conductance measurements for four different chemical linker groups. Analysis of these data show that amine, methylsulfide, and diphenylphosphine linkers break in a molecular junction with a most probable breaking force of about 0.6, 0.7, and 0.8 nN respectively. Measurements carried out with C4SH linkers, which do not show a well-defined molecular conductance signature, are analyzed directly from force traces through automated identification of force events. We find that C4SH junctions on average have more force events per trace than C4SMe. This observation supports the notion that a strong covalent S−Au bond drives more significant rearrangement of these molecular junctions. However, on average the rupture forces in C4SH junctions are smaller than the 1.4 nN rupture force for the single Au atom contact.

ASSOCIATED CONTENT

Ⓢ Supporting Information

Additional data, analysis details, and computational results. This material is available free of charge via the Internet at http://pubs.acs.org.

AUTHOR INFORMATION

Corresponding Author

mhyberts@bnl.gov; lv2117@columbia.edu

Notes

The authors declare no competing financial interest.

REFERENCES

(1) (a) Reed, M. A.; Zhou, C.; Muller, C. J.; Burgin, T. P.; Tour, J. M. *Science* **1997**, *278*, 252. (b) Reichert, J.; Ochs, R.; Beckmann, D.; Weber, H. B.; Mayor, M.; von Lohneysen, H. *Phys. Rev. Lett.* **2002**, *88*, 176804. (c) Smit, R. H. M.; Noat, Y.; Untiedt, C.; Lang, N. D.; van Hemert, M. C.; van Ruitenbeek, J. M. *Nature* **2002**, *419*, 906. (d) Xu, B. Q.; Tao, N. J. *Science* **2003**, *301*, 1221. (e) Joachim, C.; Ratner, M. A. *Proc. Natl. Acad. Sci. U.S.A.* **2005**, *102*, 8801. (f) Venkataraman, L.; Klare, J. E.; Nuckolls, C.; Hybertsen, M. S.; Steigerwald, M. L. *Nature* **2006**, *442*, 904.

(2) Frei, M.; Aradhya, S. V.; Koentopp, M.; Hybertsen, M. S.; Venkataraman, L. *Nano Lett.* **2011**, *11*, 1518.

(3) (a) Dudko, O. K.; Filippov, A. E.; Klafter, J.; Urbakh, M. *Proc. Natl. Acad. Sci. U.S.A.* **2003**, *100*, 11378. (b) Evans, E. *Annu. Rev. Biophys. Biomol. Struct.* **2001**, *30*, 105.

(4) Marszalek, P. E.; Greenleaf, W. J.; Li, H. B.; Oberhauser, A. F.; Fernandez, J. M. *Proc. Natl. Acad. Sci. U.S.A.* **2000**, *97*, 6282.

(5) (a) Parameswaran, R.; Widawsky, J. R.; Vazquez, H.; Park, Y. S.; Boardman, B. M.; Nuckolls, C.; Steigerwald, M. L.; Hybertsen, M. S.; Venkataraman, L. *J. Phys. Chem. Lett.* **2010**, *1*, 2114. (b) Park, Y. S.; Whalley, A. C.; Kamenetska, M.; Steigerwald, M. L.; Hybertsen, M. S.; Nuckolls, C.; Venkataraman, L. *J. Am. Chem. Soc.* **2007**, *129*, 15768.

(6) (a) Rubio, G.; Agrait, N.; Vieira, S. *Phys. Rev. Lett.* **1996**, *76*, 2302. (b) Rubio-Bollinger, G.; Bahn, S. R.; Agrait, N.; Jacobsen, K. W.; Vieira, S. *Phys. Rev. Lett.* **2001**, *8702*, 026101. (c) Tavazza, F.; Levine, L. E.; Chaka, A. M. *J. Appl. Phys.* **2009**, *106*, 043522.

(7) Kamenetska, M.; Koentopp, M.; Whalley, A.; Park, Y. S.; Steigerwald, M.; Nuckolls, C.; Hybertsen, M.; Venkataraman, L. *Phys. Rev. Lett.* **2009**, *102*, 126803.

(8) (a) Kresse, G.; Furthmuller, J. *Phys. Rev. B* **1996**, *54*, 11169. (b) Kresse, G.; Joubert, D. *Phys. Rev. B* **1999**, *59*, 1758. (c) Blochl, P. E. *Phys. Rev. B* **1994**, *50*, 17953. (d) Perdew, J. P.; Burke, K.; Ernzerhof, M. *Phys. Rev. Lett.* **1996**, *77*, 3865.

(9) (a) Ulrich, J.; Esrail, D.; Pontius, W.; Venkataraman, L.; Millar, D.; Doerrer, L. H. *J. Phys. Chem. B* **2006**, *110*, 2462. (b) Arroyo, C. R.; Leary, E.; Castellanos-Gómez, A. s.; Rubio-Bollinger, G.; González, M. T.; Agraït, N. s. *J. Am. Chem. Soc.* **2011**, *133*, 14313.

(10) Basch, H.; Cohen, R.; Ratner, M. A. *Nano Lett.* **2005**, *5*, 1668.

(11) (a) Kruger, D.; Fuchs, H.; Rousseau, R.; Marx, D.; Parrinello, M. *Phys. Rev. Lett.* **2002**, *89*, 186402. (b) Strange, M.; Lopez-Acevedo, O.; Hakkinen, H. *J. Phys. Chem. Lett.* **2010**, *1*, 1528. (c) Paulsson, M.; Krag, C.; Frederiksen, T.; Brandbyge, M. *Nano Lett.* **2009**, *9*, 117. (d) Li, Z.; Kosov, D. S. *Phys. Rev. B* **2007**, *76*, 035415.

(12) (a) Qi, Y. H.; Qin, J. Y.; Zhang, G. L.; Zhang, T. *J. Am. Chem. Soc.* **2009**, *131*, 16418. (b) Li, Z. L.; Zhang, G. P.; Wang, C. K. *J. Phys. Chem. C* **2011**, *115*, 15586.

(13) Xu, B. Q.; Xiao, X. Y.; Tao, N. J. *J. Am. Chem. Soc.* **2003**, *125*, 16164.

(14) Cossaro, A.; Mazzarello, R.; Rousseau, R.; Casalis, L.; Verdini, A.; Kohlmeyer, A.; Floreano, L.; Scandolo, S.; Morgante, A.; Klein, M. L.; Scoles, G. *Science* **2008**, *321*, 943.